Biomacromolecules

pubs.acs.org/Biomac

Article

Self-Fibrillating Cellulose Fibers: Rapid In Situ Nanofibrillation to Prepare Strong, Transparent, and Gas Barrier Nanopapers

Yunus Can Gorur, Per A. Larsson, and Lars Wågberg*

Cite This: *Biomacromolecules* 2020, 21, 1480−1488

Read Online

ACCESS | Metrics & More | Article Recommendations | Supporting Information

ABSTRACT: Cellulose nanofibrils (CNFs) prepared from wood biomass are promising candidates to replace oil-based materials in, for example, packaging applications. However, CNFs' affinity for water combined with their small size leads to very slow and energy-demanding processes for handling and removal of water. To a large extent, this is the major roadblock that prevents a feasible production of dry CNF-based materials on an industrial scale. In this work, self-fibrillating fibers (SFFs) from wood, where the fibrils can be liberated by external stimuli, were prepared via sequential TEMPO and periodate oxidation reactions. Papers made from these modified fibers using conventional laboratory papermaking methods were then in situ nanofibrillated via a modest pH increase. With a dewatering time of less than 10 s for a 3 g/L dispersion, SFFs represent a major improvement over conventional CNF nanopapers that take approximately 6 h to dewater. Moreover, 100 g/m^2 nanopapers obtained through in situ fibrillation exhibited comparable, if not superior, properties to those reported for conventionally made CNF films. A tensile strength of 184 MPa, a Young's modulus of 5.2 GPa, a strain at break of 4.6%, 90% optical transmittance, and an oxygen permeability of 0.7 cm^3 μm m^{-2} d^{-1} kPa^{-1} at 50% RH were measured for SFF nanopapers. Furthermore, in situ nanofibrillation of the SFFs can also be achieved from already dried papers, facilitating numerous possibilities in terms of logistics and handling for an industrial scale-up and transportation of nanomaterials. Overall, stimuli-induced SFFs indeed enable a rapid production of strong, transparent, gas barrier nanopapers, which likely can be industrially scaled up and eventually compete with the oil-based plastics in the market for packaging materials.

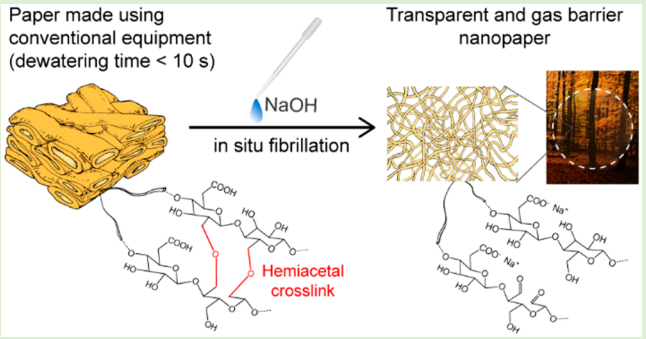

INTRODUCTION

Recent advances in science and technology in combination with an increased environmental consciousness have shifted the societal and industrial focus toward green products and sustainable processes. This new movement has been further fueled by the scarcity of oil reserves and the current disproportionate relationship between the production and recycling of plastics. As a result, there is an incentive to replace oil-based polymeric materials with renewable and biodegradable alternatives. However, considering that it is the excellent material properties and good processability of oil-based polymeric materials that established their market position, it is foreseeable that a complete replacement of these materials with their natural counterparts will not be an easy task. Good barrier properties, processability, stability, and high transparency are just some of the desired qualities for commonly used packaging materials and oil-based polymeric materials indeed provide these qualities.[1] To replace oil-based materials with renewable and bio-based materials, it is hence necessary to reach at least similar performance levels at a similar cost. One way to readily achieve this goal is to use naturally abundant biopolymers with existing industrial scale production and processing protocols. In this respect, packaging grade papers are promising candidates to facilitate this transition from nonrenewable to renewable raw materials while keeping a similar cost because papers are made of naturally sourced fibers using already existing processes in the pulp and paper industry. However, there is also a great need to improve the properties of existing materials, which likely will require a dramatic redesign of industrial processes. This is naturally beyond the scope of the current work but must be considered for the future development of bio-based packaging materials.

Besides being one of the most abundant biopolymers on Earth, cellulose attracts considerable attention due to its excellent mechanical properties, biodegradability, and renewability.[2] One of the promising new material streams of cellulose is cellulose nanofibrils (CNFs), a nanoparticle with nanoscale cross section and high aspect ratio.[3] These characteristics enable

Received: January 10, 2020
Revised: February 26, 2020
Published: March 13, 2020

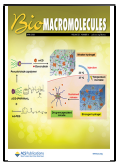

https://dx.doi.org/10.1021/acs.biomac.0c00040
Biomacromolecules 2020, 21, 1480−1488

them to be used not only as strong and transparent barrier films in packaging applications[4] but also in the advanced bottom-up engineering of complex materials structures.[5] Aside from their small size, an important feature of CNFs is their hydrophilicity, which is a great advantage for processing in aqueous media. However, this affinity for water and nanoscale dimensions result in long dewatering times and energy-demanding evaporation protocols that ultimately lead to limited CNF production at the industrial scale. Furthermore, commonly used charge-introducing pretreatments, such as carboxymethylation or other oxidation routes to introduce carboxyl groups, used to facilitate nanofibrillation extend dewatering times even further (more than 10 times compared to uncharged CNFs) due to an increased specific water-absorption behavior of the modified cellulose.[6] In general, smaller fibril dimensions lead to better material properties at the expense of longer processing times. To escape from this impasse, numerous research groups have used nontraditional processing methods, such as the use of ionic liquids,[7] introducing a range of fiber sizes[8] or utilizing hot pressing[9] to assist the dewatering process. Nonetheless, these methods all have their respective shortcomings, either from an environmental, practical, or performance point of view.

The novel method described in the present work overcomes many of these challenges by utilizing conventional papermaking methods combined with well-established, water-based chemical modification techniques followed by nanofibrillation of an already formed paper via a modest pH increase. Delaying nanofibrillation of the fibers until after sheet forming effectively eliminates long dewatering times, yet still provides the excellent properties of a CNF nanopaper. The fiber treatment procedures involve a careful manipulation of the fiber wall properties by a combination of 2,2,6,6-tetramethyl-1-piperidineyloxy (TEMPO) modification and periodate oxidation that yield stimuli-induced self-fibrillating fibers (SFFs) without sacrificing the rate of dewatering or the desired properties. The effect of the chemical modification on the fiber morphology, degree of fibrillation, and dewatering rate of SFFs are carefully studied and quantified. Finally, the nanopapers made from SFFs are characterized in terms of their mechanical, barrier, and optical properties. The unique combination of chemical treatments presented in this work is simple, robust, and fast, opening up numerous possibilities for a future industrial scale-up.

MATERIALS AND METHODS

Materials. Fully bleached, never-dried, softwood kraft pulp fibers were obtained from BillerudKorsnäs AB (Gruvön pulp mill, Grums, Sweden). The fibers were industrially beaten (114 kW h/t) and had a water retention value of 1.98 g/g. The chemicals used for the reactions sodium hypochlorite (10−15% solution), 2,2,6,6-tetramethyl-1-piperidineyloxy (TEMPO, free radical), sodium bromide, sodium (meta)-periodate (99%), 2-propanol (99.9%) were all purchased from Sigma-Aldrich and were used as received. Sodium hydroxide and hydrochloric acid standard solutions (1 M) were obtained from Merck Millipore.

Preparation of SFFs. TEMPO oxidation of the fibers was performed in alkaline media in order to predominantly introduce carboxyl groups to the C6 position on cellulose.[6] Amounts of 0.1 mmol TEMPO, 1 mmol NaBr, and 9.7 mmol NaClO per gram of dry fiber were added to a 12 g/L fiber suspension and kept to react for 1.5 h under gentle stirring at room temperature. The reaction pH was maintained at 10.5 by dropwise addition of 0.5 M NaOH to the suspension. For the periodate oxidation of the TEMPO-oxidized pulp, 5.4 g of sodium periodate was added per gram of dry fiber to a 12 g/L fiber suspension under gentle stirring, which also contained 6.3 vol % 2-propanol as radical scavenger to prevent side reactions.[10] The fibers were oxidized for 1.5 h at 70 °C in the dark to further limit side reactions. Periodate oxidation was also performed at room temperature using similar chemical and material loadings for 24 h. Both reactions were terminated by filtering off the chemicals followed by thorough washing with deionized water.

Chemical Characterization of SFFs. The total charge of the fibers was determined via conductometric titration using a Metrohm 702SM Titrino titrator according to the SCAN-CM 65:02 standard. Each measurement was performed in triplicates.

The aldehyde content was determined by titration with NaOH after reaction with hydroxylamine, which reacts with the aldehydes to release a stoichiometric amount of protons.[11] Each measurement was performed in triplicates.

Fourier transform infrared spectrometry (FTIR) of the modified fibers in their protonated forms was performed using a PerkinElmer Spectrum 100 FTIR equipped with a diamond attenuated total reflection crystal (Gaseby Specac Ltd, UK). The spectra were recorded at room temperature taking the average of eight scans with 4 cm^{-1} resolution in the range of 600−4000 cm^{-1}.

Measuring the Level of Fibrillation in SFFs. In order to quantify the amount of nanofibrillation taking place in different samples, a simple protocol was developed. The test was based on the assumption that truly liberated CNFs are colloidally stable and hence do not sediment when centrifuged from a dispersed state. A 200 mL fiber suspension with a consistency of 1 g/L was brought to pH 12, evenly divided into five conical Falcon tubes and centrifuged at 4120 RCF for 1 h in an Avanti J-E Centrifuge (Beckman Coulter, Brea, CA, USA). The supernatant was decanted from the tubes, and the sediment was filtered using a 0.65 μm DVPP membrane (Merck Millipore, Burlington, MA). Samples were weighed following oven drying. Finally, the degree of fibrillation was calculated as the mass fraction of the total that was found in the supernatant.

Atomic Force Microscopy. A MultiMode 8 atomic force microscope (AFM, Bruker, Santa Barbara, CA, USA) was used to characterize the fibril dimensions after nanofibrillation. The supernatant from the centrifuged CNF dispersions was adsorbed on a polyvinylamine-treated silica wafer. Imaging was performed in ScanAsyst mode with a cantilever that has nominal-tip radius of 2 nm over a 5 × 5 μm^2 scanning area.

Preparation of SFF Papers and Nanopapers. Paper sheets with a target grammage of 100 g/m^2 were prepared using a vacuum filtration setup equipped with a standard Rapid Köthen sheet former (Paper Testing Instruments, Austria) wire. The pulp suspension was protonated at pH 2 for 10 min in order to ensure that the fibers were in the deswollen state prior to sheet forming. Once the paper was formed and removed from the forming wire, nanofibrillation was achieved via immersion in a pH 12 sodium hydroxide solution, forming a wet nanopaper. Alternatively, the SFF paper was dried at a temperature of 93 °C and a reduced pressure of 95 kPa for 12 min, followed by immersion in a pH 12 sodium hydroxide solution to achieve fibrillation.

Morphology of Papers and Nanopapers. To obtain cross-sectional and top views of the "wet" structure of the papers, supercritical carbon dioxide drying was used to prevent a collapse of the wet network structure during drying. This made it possible to capture images of the inter- and intrafibrillar morphology of the paper under conditions that are closest to the swollen state. The formed sheets were solvent exchanged to ethanol, first by placing them in an ethanol bath (96%) and subsequently in pure ethanol (99.8%) for 10 min each. The solvent-exchanged samples were then placed in a critical point dryer chamber (Autosamdri-815, Tousimis, MD, USA), and liquid carbon dioxide was injected into the chamber under a pressure of 55 bar to displace the ethanol. The chamber was then brought above the critical point of carbon dioxide (100 bar and 40 °C). The chamber was isothermally depressurized, and carbon dioxide was evaporated without significant collapse of the paper structure. A Hitachi S-4800 high-resolution field-emission scanning electron microscope (SEM) was used to obtain images of the papers and nanopapers. To minimize specimen charging during imaging, samples were coated with a thin layer of platinum−palladium in a 208 HR Cressington Sputter Coater. Cross sections of

https://dx.doi.org/10.1021/acs.biomac.0c00040
Biomacromolecules 2020, 21, 1480−1488

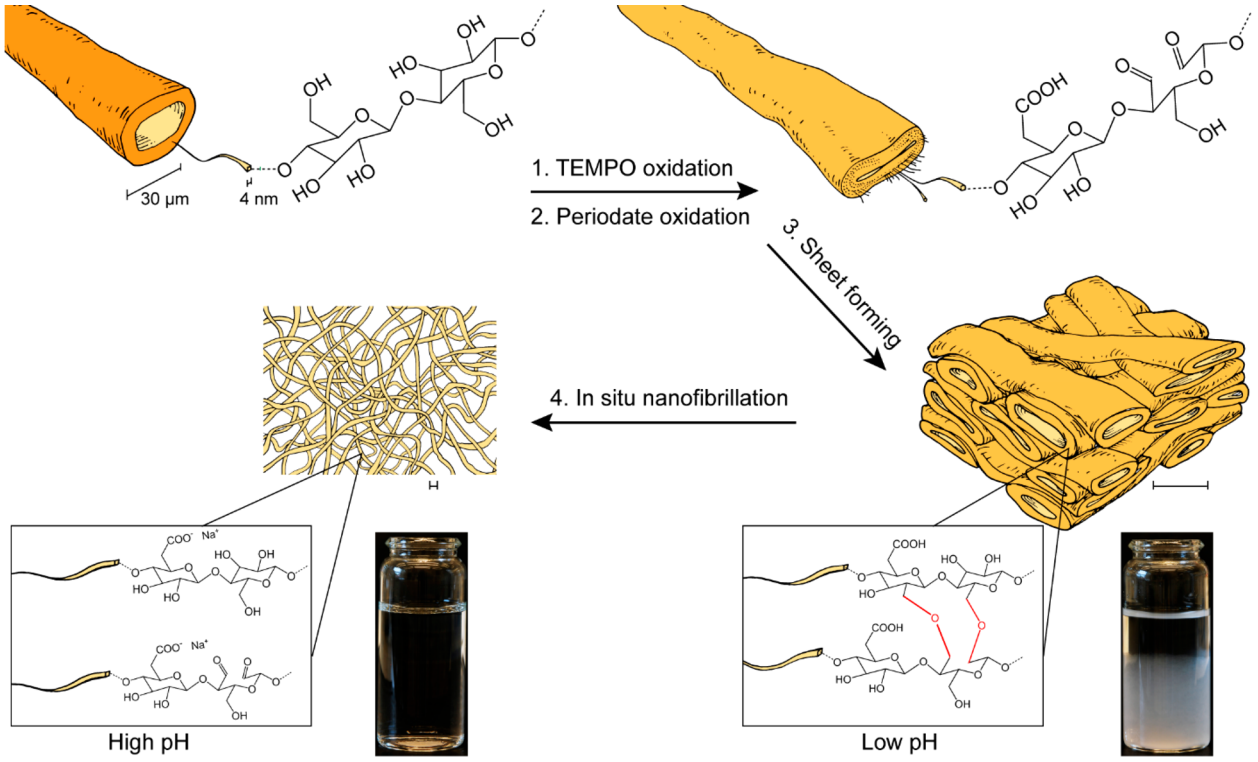

Figure 1. Scheme of sequential TEMPO and periodate oxidation followed by sheet forming and subsequent in situ nanofibrillation in the formed sheet. The inset photographs of vials represent SFF dispersions before and after stimuli-induced nanofibrillation.

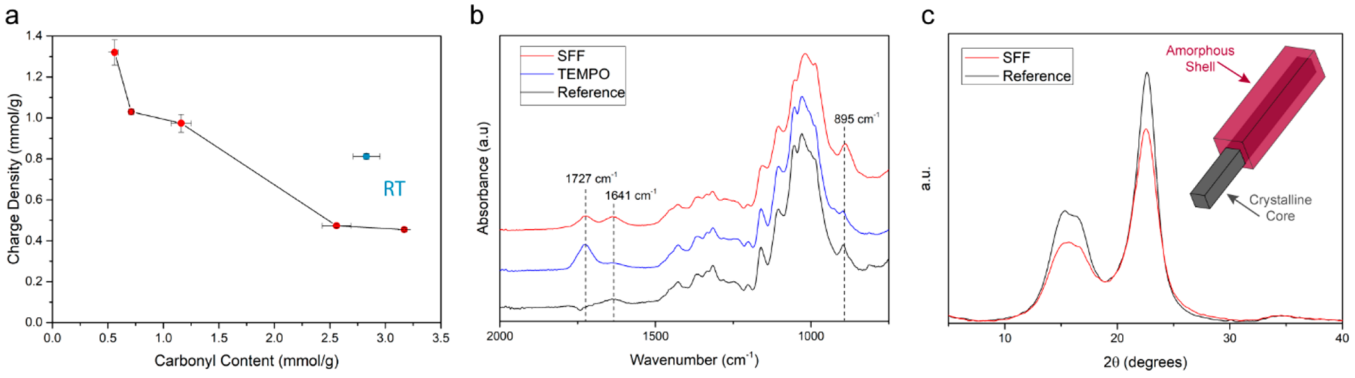

Figure 2. (a) Charge density evolution of SFFs with respect to carbonyl content, sample named RT in blue represents the room temperature oxidized sample. (b) FTIR spectra showing the introduction of respective chemical groups onto cellulose molecules. (c) XRD diffractograms of unmodified cellulose and SFFs with the schematic of the "core−shell" structure in the inset.

samples were prepared by fracturing the samples after freezing in liquid nitrogen.

X-ray Diffraction. The supramolecular order in the modified fibers was evaluated by acquiring their X-ray diffraction (XRD) patterns using an X'Pert Pro XRD (PANalytics, Netherlands) with Cu Kα radiation generated at 45 kV and 40 mA in the angular range of 5−40° (2θ). Crystallinity was calculated by peak deconvolution where the broad amorphous peak was located at approximately 21.5° and all individual crystalline peaks were fitted until an iteration with an R^2 value of 0.997 was reached.[12,13] The crystallite width was calculated using the Scherrer formula on the (002) lattice peak, assuming a shape factor of 0.9.[14]

Mechanical Properties. Tensile tests were performed on test pieces that were 5 mm wide and 70−100 μm thick, using an Instron 5944 universal testing system, equipped with a 500 N load cell, in a controlled climate of 23 °C and 50% RH. Samples were clamped with a free span of 30 mm and strained at a rate of 3 mm/min. The strain was determined by measuring the grip displacement, and the Young's modulus was calculated as the slope of the stress−strain curve in the linear region at the 0.5−1% interval. A total of 10 test pieces were tested per sample.

Oxygen Barrier Properties. The oxygen permeability was measured for 5 cm^2 samples using a MOCON OX-TRAN 2/21 according to the ASTM D3985 and ASTM F1927 standards. The oxygen permeability measurements were performed at 23 °C and 50% RH or 80% RH, using the same relative humidity on both sides of the sample. The measurements were performed in duplicates.

Optical Properties. The optical properties of the nanopapers were measured using a Shimadzu UV-2550 UV−vis spectrophotometer equipped with an integrating sphere accessory. Measurements were taken at three random points on each sample and measurements were performed in triplicates.

RESULTS AND DISCUSSION

Chemical Characterization of SFFs. Mechanically beaten fibers were chemically modified according to Figure 1 to obtain SFFs, which were later in situ nanofibrillated. First, TEMPO

https://dx.doi.org/10.1021/acs.biomac.0c00040
Biomacromolecules 2020, 21, 1480−1488

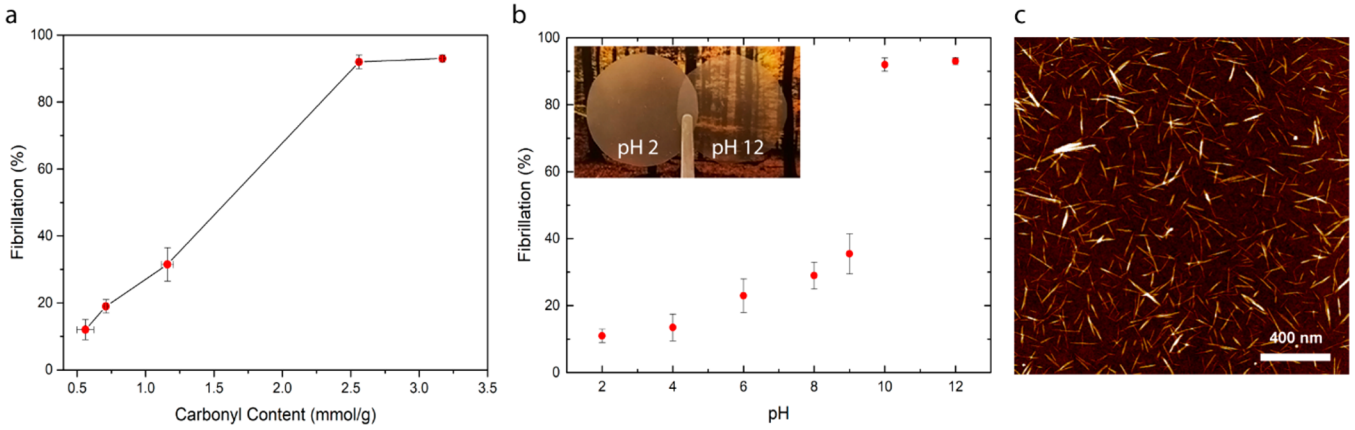

Figure 3. (a) Fibrillation percentage of modified fibers with respect to carbonyl content. (b) Fibrillation percentage of SFFs (charge density of 0.49 mmol/g, aldehyde content of 3.17 mmol/g) with respect to pH. The inset image shows films made at different pH values, photographed at a height of 10 mm above the image. (c) AFM image of SFFs fibrillated at pH 12.

oxidation was performed in order to introduce carboxyl groups in the C6 position of the glucose unit. Charges were introduced to facilitate swelling and to separate the CNFs constituting the fiber wall, without completely liberating them into free fibrils. This fibril separation additionally opens up the fiber wall to expose more fibril surfaces to further chemical modifications.[15] Subsequently, periodate oxidation, which introduces aldehydes by opening the anhydroglucose ring in the C2−C3 positions,[10] was performed. Besides introducing aldehydes that can form hemiacetals with adjacent hydroxyl groups at low and neutral pH, periodate oxidation has been shown to be able to oxidize also the glucose units found under the external layer of cellulose in the fibrils, thereby altering the supramolecular structure of the fibrils, fibril aggregates, and finally fiber wall.[11,16]

The total charge and carbonyl content of the modified fibers were determined by conductometric titration and reaction with hydroxylamine hydrochloride, respectively. After the TEMPO oxidation in alkaline media, the total charge of the fibers reached approximately 1.3 mmol/g along with a carbonyl content of 0.5 mmol/g, which was in accordance with earlier findings.[6] Subsequent periodate oxidation increased the carbonyl content while lowering the total charge. This trend continued until a carbonyl content of approximately 2.5 mmol/g was reached. Beyond this point, further periodate oxidation did not lower the total charge significantly, yet the carbonyl content continued to rise (Figure 2a). Reduction of charge following periodate oxidation has been ascribed to material loss due to surface peeling of modified cellulose.[17−19]

FTIR spectra of the protonated forms of unoxidized, TEMPO-oxidized, and SFFs are shown in Figure 2b. The spectrum of TEMPO oxidized cellulose shows a characteristic band near 1720 cm^{-1}, which is assigned to the protonated forms of the carboxyl groups and is consequently not seen in the spectrum of the unoxidized cellulose sample.[20] A further periodate oxidation of TEMPO oxidized cellulose leads to the appearance of a characteristic aldehyde carbonyl group at approximately 1640 cm^{-1} along with a strengthening of the band at 895 cm^{-1}, assigned to the hydrated forms of aldehyde groups.[20] The fact that the carbonyl peak intensity being rather low considering the extent of modification performed for the fibers can be attributed to the aldehydes preferring to form hemiacetal linkages rather than staying in their free form.[16] Furthermore, it was observed that the intensity of the carboxyl band in TEMPO-oxidized cellulose was lowered following consecutive periodate oxidation, which is in accordance with the total charge and carbonyl contents determined in this study along with the earlier presented results.[17,21] The presumption about the peeling and dissolution of surface carboxyl groups was further supported when the periodate oxidation was conducted at room temperature instead of at 70 °C in order to limit degradation and dissolution of modified cellulose. It was observed that not only the remaining material after the reaction showed a higher gravimetric yield but also more of the carboxyl groups previously introduced via TEMPO-oxidation were retained (Figure 2a). Although the total charge measured after high-temperature periodate oxidation showed an approximately 60% decrease compared to the original TEMPO-oxidized material, this value was under 30% for fibers that were periodate oxidized at room temperature. Similar observations regarding the dissolution of periodate-oxidized cellulose at high temperature further supports this view.[22]

Analysis of X-ray diffractograms of SFFs shows decreased crystallinity and crystallite size following chemical modifications (Figure 2c and Table S1), which is in accordance with changes to both charge and carbonyl content as well as previous findings.[10,23] It is often reported in the literature that periodate oxidation leads to a lowering of the cellulose crystallinity.[24,25] Because this oxidation is a heterogeneous reaction involving one solid species and one dissolved species, it will first predominantly affect the surface of the CNF aggregates and the nanofibrils.[26] Eventually, the reaction will make its way toward the interior of the fibril, resulting in a "core−shell" structure, where the crystalline core is surrounded by a highly derivatized nonordered outer layer (inset in Figure 2c).[27,28] This is suggested to be one of the main contributions to the stimuli-induced self-fibrillation mechanism, which will be discussed in detail later.

pH-Induced Fibrillation of SFFs. Fibers modified to different degrees were studied, and their fibrillation levels were correlated with different degrees of oxidation as well as their fibrillation behavior under different pH conditions. To investigate this correlation, a protocol to measure the level of fibrillation, as described in the experimental section, was used. This method, in short, utilized the assumption that charged CNFs are colloidally stable and hence do not sediment when subjected to centrifugation.

As shown in Figure 3a, the increase in fibrillation was rather limited until a carbonyl content of about 1.2 mmol/g was

https://dx.doi.org/10.1021/acs.biomac.0c00040
Biomacromolecules 2020, 21, 1480−1488

reached, which corresponds to a degree of oxidation of about 10% (assuming that all cellulose molecules are available for modification). For this level of modification, periodate oxidation is likely predominantly occurring on the external surfaces of the nanofibrils. As the level of periodate oxidation increases, further alteration of the crystalline structure will occur and contribute to a steady increase in the amount of fibrillation.[21,29] These observations further indicate that periodate oxidation, at least in the beginning, is essentially a surface derivatization and does not affect the structure of the nanofibrils in the fiber wall until a critical point is passed. Oxidation beyond this critical point, which is reported to be between 15 and 20% degree of oxidation,[16] leads to the disturbance of the ordered microstructure in the fibers to such a significant extent that CNFs can be liberated completely with the minimum amount of chemical stimuli. Indeed, at a carbonyl content of 2.6 mmol/g (corresponding to 21% degree of cellulose oxidation), about 92% fibrillation was achieved by a simple pH increase. At this degree of oxidation, increasing the pH breaks the hemiacetal bonds formed at lower pHs in the fiber wall and liberates the fibrils, thus disintegrating the fiber wall.[30,31]

Figure 3b shows the fibrillation of SFFs modified to a carbonyl content of 3.2 mmol/g (corresponding to 26% degree of oxidation) upon gentle agitation over a pH range of 2−12. Based on these results the fibrillation behavior of SFFs could be divided into three different regimes: nonfibrillating regime (pH 2−4), intermediate regime (pH 4−9), and fully fibrillating regime (pH 9−12). In the pH 2−4 interval, the fibrillation level was below 15%, and insignificant fibrillation was observed with increasing pH, even though the pK_a of carboxylic acids is approximately 4. This can however be attributed to the fact that the pH is lower inside the fiber wall than the bulk solution due to the Donnan effect.[32] Therefore, the low pH not only reduces the osmotic pressure induced swelling within the fiber wall but also maintains the hemiacetal cross-links, thus making fibrillation more difficult. In the intermediate regime, pH 6−9, the fibrillation showed a significant increase, ranging between 20 and 30%. While the total degree of fibrillation is low, the effects of pH with respect to fibrillation are more pronounced, indicating the beginning of a significant swelling for the modified fibers. However, despite the significant swelling due to charging of the carboxyl groups, the hemiacetal cross-links maintain fiber wall integrity and limit fibrillation. Upon reaching pH 10, an almost complete fibrillation was achieved due to the simultaneous swelling and breaking of hemiacetal cross-links. At pH 10, the level of fibrillation was 92% and a further increase of the pH to 12 did not have any significant effect on the fibrillation. The effect of pH on the fibrillation was emphasized further when films were prepared with conventional methods using CNFs prefibrillated at different pH values (inset in Figure 3b).

The dimensions of the CNFs produced by the self-fibrillation method was determined by AFM analysis after their adsorption on silica wafers (Figure 3c). Although CNFs from SFFs are shorter than conventional CNFs, similar observations have been made for CNFs produced after similar chemical treatments.[33−35] Aside from a decreased degree of polymerization due to TEMPO and periodate oxidation,[36] an important factor contributing to the shortening of the fibrils is presumed to be the alkaline degradation of periodate oxidized cellulose during the alkali-mediated nanofibrillation process. This happens because the dialdehyde modified cellulose is more sensitive to alkaline degradation than nonmodified cellulose.[19] It is anticipated that further optimization of the alkali-mediated nanofibrillation process will allow for better retention of CNF length.

Stimuli-Induced Self-Fibrillation Phenomenon and Its Contributing Factors. The swelling of a cellulose fiber wall can be described as the swelling of a polyelectrolyte gel[37,38] and therefore the methods used for describing the swelling of these systems can be used to describe the swelling behavior of the fiber wall. The swelling of a charged hydrogel is described by three different pressure terms: the ionic contribution (π_{ion}) that is the osmotic pressure created by the immobile carboxyl groups inside the fiber wall, the gel-solvent mixing contribution (π_{mix}) that is the osmotic pressure due to the free energy of mixing between cellulose and water, and the network pressure contribution (π_{def}) that is the osmotic pressure due to a change in free energy caused by a deformation of the network, all of which make up the total swelling pressure (π_{tot}) in the network.[32]

$$\pi_{tot} = \pi_{ion} + \pi_{mix} + \pi_{def} \quad (1)$$

Although these swelling and restraining forces remain in balance inside the fiber wall, changing the equilibrium state by increasing or decreasing these terms significantly will result in a swelling or deswelling of the system. In the case of SFFs, introduction of charges via TEMPO oxidation contributes to the swelling forces π_{ion}, which depends on the ionic strength and pH inside the fiber wall, and π_{mix}, which is the willingness of the cellulose to interact with water rather than with itself. On the other hand, an increase in π_{ion} alone is not enough to overcome the restraining forces. Therefore, the subsequent periodate oxidation is performed, which serves two main purposes; first is to disturb the supramolecular structure and decrease restraining forces, π_{def}, and second is to introduce aldehydes inside the fiber wall, which will create hemiacetal linkages that will prevent the liberation of fibrils from the fiber wall under low pH conditions. It is well known that the presence of carbonyl groups in the close vicinity of alcohols facilitates the formation of covalent bonds such as hemiacetals.[39,40] The formation of hemiacetals cross-link the fiber wall at lower pH, making it more rigid. In the case of cellulose, the aldehyde groups formed in C2 and C3 positions as a result of periodate oxidation make way for these cross-links.[41] The linkages are both inter- and intramolecular in nature, and they are stable at lower pH values; however, they rapidly decompose under alkaline conditions.[16,18,42]

Because increasing the swelling forces by introduction of charges and decreasing restraining forces by disturbing the supramolecular structure tips the balance in favor of swelling, the fiber wall becomes extremely susceptible to outside stimuli such as pH. By increasing the pH, swelling forces are further increased and the hemiacetal linkages, which are the last factor contributing to the restraining forces, are eliminated, resulting in extensive swelling and eventual liberation of the fibrils. Nonetheless, it should be stressed that neither charge introduction nor aldehyde introduction alone creates the conditions required for pH-induced self-fibrillation. When SFFs are suspended in a dispersion with high sodium chloride content, the fibrillation does not take place even when the pH is brought close to 13 because of the screening of charges that prevents the osmotic pressure induced swelling. However, upon dilution of the suspension with deionized water and eliminating screening, fibrillation takes place. This further supports the inferences made regarding the cooperative action of charge and aldehydes in the stimuli-induced self-fibrillation phenomenon observed.

https://dx.doi.org/10.1021/acs.biomac.0c00040
Biomacromolecules 2020, 21, 1480−1488

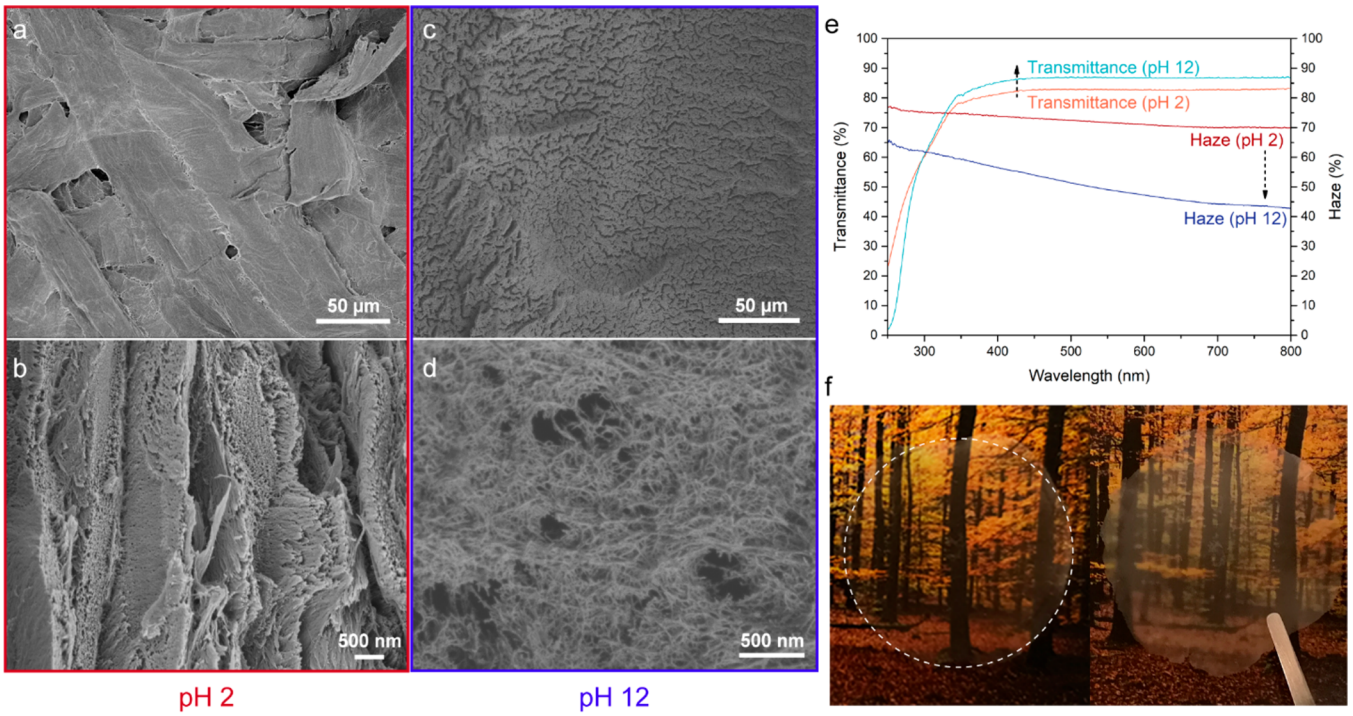

Figure 4. (a,b) SEM images, top-view and cross section, respectively, of a paper made with unfibrillated SFFs and (c,d) the same paper after pH induced in situ fibrillation. (e) Transmittance and haze measurements of SFF papers before and after fibrillation. (f) Photographs of SFF nanopapers after fibrillation; placed on a surface (left) and held 10 mm above the same surface (right).

Table 1. Dewatering Times for the Fabrication of Nanopapers and Their Respective Physical, Mechanical, Barrier, and Optical Properties

refs	starting material	dewatering time (min)	dry thickness (μm)		dry density (g/cm^3)	tensile strength (MPa)	Young's modulus (GPa)	strain at break (%)	O_2 permeability (cm^3 μm m^{-2} d^{-1} kPa^{-1}) 50% RH	O_2 permeability (cm^3 μm m^{-2} d^{-1} kPa^{-1}) 80% RH	T^a (%)
43	CNFs	>1 day	100		1.51	178	10	5.1	0.049		87
44	MFCs	>1 day	20		0.811	104	15.7	5.3	3.52		
45	MFCs	>1 day	5		1.57				0.85	10.5	90
46	CNFs	480	20		1.46	233	6.9	7.6			90
9	CNFs	60	120		1.25	121	8.1	7.9	0.6	12.5	
47	CNFs	45	60		1.29	152	9.26				85
48	MFCs	45	40		1.40	232	13.4	5.0			42
7	MFC	10	60		0.85	121		15.2			91
49, 50	CNFs	9	43		1.40	148	11.1	2.02	1.5	2.2	
51	MFC	2	42		0.47	35		5.5			82
this work	SFFs	0.17	unfibrillated	105	1.29	114	4.4	2.9	1.6	8.4	83
			fibrillated	70	1.40	184	5.2	4.6	0.7	2.4	90

[a]Transmittance measured at 600 nm.

Preparation of SFF Papers, Their In Situ Fibrillation, and Resulting Nanopaper Properties. The efficiency of the nanopaper making process is essentially a trade-off between the preparation time and final nanopaper properties. SFFs overcome this trade-off situation while retaining the desired final properties and a high dewatering speed by strategically manipulating the behavior of the fiber wall under different conditions. When SFFs were used to make papers to be fibrillated via external stimuli, sheets were formed with conventional papermaking equipment at high dewatering speed and at a minimum material loss. Sheets were formed at moderately low pH values, since then hemiacetals are formed, holding the fiber wall together despite the cumulative softening caused by the previous chemical modifications. This prevents the fiber wall from falling apart and thereby slipping through the formation wire. Once the sheet forming was completed, the sample could be exposed to a higher pH that would synergistically cause swelling and hydrolyze the hemiacetal linkages, thus disintegrating the fiber wall to form a CNF gel.[11] The effects of stimuli-induced self-fibrillation become even more apparent by analyzing the SEM images of critical-point-dried films before and after fibrillation, which show distinct differences in terms of fiber morphology and surface topography (Figure 4a–d). An unfibrillated sample prepared at low pH exhibits typical fiber-like structures, similar to conventionally made paper (Figure 4a,b). On the other hand, the fibrillated sample

https://dx.doi.org/10.1021/acs.biomac.0c00040
Biomacromolecules 2020, 21, 1480−1488

shows completely different morphology, with no evidence of macroscopic fiber structures (Figure 4c). Moreover, it is possible to see individual liberated nanofibrils within the dense network of the fibrillated gel, whereas these structures are absent in the unfibrillated sample (Figure 4d).

The forming of a sheet with a typical dry thickness of 100 μm (a grammage of about 120 g/m^2)and a consecutive pH-induced nanofibrillation to a nanopaper takes less than 3 min (10 s of filtration and approximately 2 min for pH adjustment). After 12 min of drying under a reduced pressure of 95 kPa and a temperature of 93 °C, the resulting nanopaper exhibits comparable optical, mechanical, and barrier properties to those reported in the literature for nanopapers formed directly from CNFs, even though the SFF nanopaper was prepared significantly faster. Films made with SFFs were strong, transparent, and exhibited good barrier properties in comparison to the previously reported values (Table 1).

The papers made from unfibrillated SFFs exhibited similar mechanical properties to those prepared with dialdehyde cellulose fibers, that is, periodate oxidation only. Unfibrillated SFF papers exhibited good mechanical properties compared to unmodified cellulose; a tensile strength of 114 ± 19 MPa, a Young's modulus of 4.4 ± 0.3 GPa, and a strain at break of 2.9 ± 0.6%, which was in agreement with available studies on the cross-linking of cellulose.[11,49] However, even with the slightly increased brittleness, unfibrillated SFF sheets still exhibited values comparable to what has previously been reported in the literature. Table 1 shows that the SFF papers exhibited high transparency along with very good barrier properties with a very low oxygen permeability. Upon fibrillation of the fibers in the sheet to a CNF film, all of the properties showed substantial improvement compared to the unfibrillated counterpart; where the fibrillated nanopapers exhibited a tensile strength of 184 ± 17 MPa and a Young's modulus of 5.2 ± 0.7 GPa along with a strain at break of 4.6 ± 0.6%. Furthermore, an increased optical transparency and a lowered haze were observed (Figure 4e,f and Table S2). Likewise, the gas barrier performance of the fibrillated material was further improved compared to its unfibrillated counterpart (Table 1). These results indicate that using SFFs, nanopapers can be produced at much higher rates without having to significantly sacrifice performance. Moreover, the pH-induced nanofibrillation can be performed also for dried SFF sheets to improve the performance even further by densifying the structure, which creates interesting possibilities in terms of logistics for a future commercialized nanopaper.

Finally, SFFs can be prepared using other chemistries as well. Although results may differ to a certain extent, charge introduction can be performed via carboxymethylation or phosphorylation reactions, which both produce SFFs when subsequent peridoate oxidation is performed. Similarly, if periodate oxidation is performed first to oxidize C2−C3 secondary alcohols to aldehydes, they can then be partially chlorite oxidized or sulfonated using bisulphite to introduce charges.[24,52] These findings, which are described thoroughly in European patent application EP19175205.4-1102, support the initial assessment explaining the cooperative action of charges and hemiacetals, where regardless of the chemistry, introduction of any type of chargeable moiety in combination with aldehydes will result in fibers that can be fibrillated upon mild alkali addition.

CONCLUSIONS

Wood-sourced cellulose-rich fibers were chemically modified using sequential TEMPO and periodate oxidation protocols in order to obtain stimuli-responsive SFFs. This stimuli-induced self-fibrillation phenomenon was attributed to the cooperative action of chargeable moieties and aldehydes capable of forming hemiacetals, which simultaneously led to the creation of an increased osmotic pressure and disturbance of the supramolecular structure, enabling stimuli-induced fibrillation of the fiber wall. Such modified fibers can be used to rapidly produce strong, transparent and gas barrier nanopapers using conventional papermaking methods. Dry sheets, which can be produced with a dewatering time of less than 10 s, exhibit satisfactory properties even before nanofibrillation, which can be further improved by stimuli-induced nanofibrillation. In this study, this was demonstrated by nanopapers exhibiting comparable mechanical (a tensile strength of 184 ± 17 MPa, a Young's modulus of 5.2 ± 0.7 GPa, a strain at break of 4.6 ± 0.6%), optical (90% total transmittance), and barrier (an oxygen permeability of 0.69 cm^3 μm m^{-2} d^{-1} kPa^{-1} at 50% RH) properties to what has been reported previously in the literature for nanopapers made from CNFs that were individualized before sheet fabrication, but with a much shorter dewatering time. Moreover, the possibility to obtain SFFs using different chemistries and the ability to perform nanofibrillation of dry papers combined with the versatility of the carbonyl groups that can act as a strong and diverse platform for further chemical modification protocols also add to the industrial relevance of this novel high-performance cellulose material. Stimuli-induced SFFs open numerous possibilities in the quest for replacing nonsustainable oil-based plastics used in high volume applications, such as packaging, without sacrificing production speed, established infrastructure or performance.

ASSOCIATED CONTENT

Supporting Information

The Supporting Information is available free of charge at https://pubs.acs.org/doi/10.1021/acs.biomac.0c00040.

Crystallinity index and crystallite size values of unmodified and modified fibers and optical transmittance and haze values of SFF papers before and after fibrillation (PDF)

Pulp fibers on demand via a simple pH modification (ZIP)

AUTHOR INFORMATION

Corresponding Author

Lars Wågberg − *Fibre and Polymer Technology, KTH Royal Institute of Technology SE-10044 Stockholm, Sweden;* orcid.org/0000-0001-8622-0386; Email: wagberg@kth.se

Authors

Yunus Can Gorur − *Fibre and Polymer Technology, KTH Royal Institute of Technology SE-10044 Stockholm, Sweden;* orcid.org/0000-0003-0519-7917

Per A. Larsson − *Fibre and Polymer Technology, KTH Royal Institute of Technology SE-10044 Stockholm, Sweden;* orcid.org/0000-0002-7410-0333

Complete contact information is available at: https://pubs.acs.org/10.1021/acs.biomac.0c00040

https://dx.doi.org/10.1021/acs.biomac.0c00040
Biomacromolecules 2020, 21, 1480−1488

Notes

The authors declare no competing financial interest.

■ ACKNOWLEDGMENTS

This work has been carried out within the national platform Treesearch and is funded through the strategic innovation program BioInnovation, a joint effort by Vinnova, Formas and the Swedish Energy Agency. L.W. also acknowledges The Knut and Alice Wallenberg foundation for the financial support though the Wallenberg Wood Science Centre. The authors would also like to thank Dr. Michael Reid for linguistic review.

■ REFERENCES

(1) Siracusa, V.; Rocculi, P.; Romani, S.; Rosa, M. D. Biodegradable Polymers for Food Packaging: A Review. *Trends Food Sci. Technol.* **2008**, *19*, 634−643.
(2) Siró, I.; Plackett, D. Microfibrillated Cellulose and New Nanocomposite Materials: A Review. *Cellulose* **2010**, *17*, 459−494.
(3) Isogai, A. Wood Nanocelluloses: Fundamentals and Applications as New Bio-Based Nanomaterials. *J. Wood Sci.* **2013**, *59*, 449−459.
(4) Abdul Khalil, H. P. S.; Bhat, A. H.; Ireana Yusra, A. F. Green Composites from Sustainable Cellulose Nanofibrils: A Review. *Carbohydr. Polym.* **2012**, *87*, 963−979.
(5) Klemm, D.; Kramer, F.; Moritz, S.; Lindström, T.; Ankerfors, M.; Gray, D.; Dorris, A. Nanocelluloses: A New Family of Nature-Based Materials. *Angew. Chem., Int. Ed.* **2011**, *50*, 5438−5466.
(6) Saito, T.; Kimura, S.; Nishiyama, Y.; Isogai, A. Cellulose Nanofibers Prepared by TEMPO-Mediated Oxidation of Native Cellulose. *Biomacromolecules* **2007**, *8*, 2485−2491.
(7) Chen, J.; Han, X.; Fang, Z.; Cheng, F.; Zhao, B.; Lu, P.; Li, J.; Dai, J.; Lacey, S.; Elspas, R.; et al. Rapid Dissolving-Debonding Strategy for Optically Transparent Paper Production. *Sci. Rep.* **2016**, *5*, 17703.
(8) Varanasi, S.; Batchelor, W. J. Rapid Preparation of Cellulose Nanofibre Sheet. *Cellulose* **2013**, *20*, 211−215.
(9) Österberg, M.; Vartiainen, J.; Lucenius, J.; Hippi, U.; Seppälä, J.; Serimaa, R.; Laine, J. A Fast Method to Produce Strong NFC Films as a Platform for Barrier and Functional Materials. *ACS Appl. Mater. Interfaces* **2013**, *5*, 4640−4647.
(10) Larsson, P. A.; Berglund, L. A.; Wågberg, L. Highly Ductile Fibres and Sheets by Core-Shell Structuring of the Cellulose Nanofibrils. *Cellulose* **2014**, *21*, 323−333.
(11) Larsson, P. A.; Gimåker, M.; Wågberg, L. The Influence of Periodate Oxidation on the Moisture Sorptivity and Dimensional Stability of Paper. *Cellulose* **2008**, *15*, 837−847.
(12) Park, S.; Baker, J. O.; Himmel, M. E.; Parilla, P. A.; Johnson, D. K. Cellulose Crystallinity Index: Measurement Techniques and Their Impact on Interpreting Cellulase Performance. *Biotechnol. Biofuels* **2010**, *3*, 10.
(13) Yang, X.; Berthold, F.; Berglund, L. A. High-Density Molded Cellulose Fibers and Transparent Biocomposites Based on Oriented Holocellulose. *ACS Appl. Mater. Interfaces* **2019**, *11*, 10310−10319.
(14) Langford, J. I.; Wilson, A. J. C. Scherrer after Sixty Years: A Survey and Some New Results in the Determination of Crystallite Size. *J. Appl. Crystallogr.* **1978**, *11*, 102−113.
(15) Sjöstedt, A.; Wohlert, J.; Larsson, P. T.; Wågberg, L. Structural Changes during Swelling of Highly Charged Cellulose Fibres. *Cellulose* **2015**, *22*, 2943−2953.
(16) Guigo, N.; Mazeau, K.; Putaux, J.-L.; Heux, L. Surface Modification of Cellulose Microfibrils by Periodate Oxidation and Subsequent Reductive Amination with Benzylamine: A Topochemical Study. *Cellulose* **2014**, *21*, 4119−4133.
(17) López Durán, V.; Larsson, P. A.; Wågberg, L. Chemical Modification of Cellulose-Rich Fibres to Clarify the Influence of the Chemical Structure on the Physical and Mechanical Properties of Cellulose Fibres and Thereof Made Sheets. *Carbohydr. Polym.* **2018**, *182*, 1−7.
(18) Erlandsson, J.; Pettersson, T.; Ingverud, T.; Granberg, H.; Larsson, P. A.; Malkoch, M.; Wågberg, L. On the Mechanism behind Freezing-Induced Chemical Crosslinking in Ice-Templated Cellulose Nanofibril Aerogels. *J. Mater. Chem. A* **2018**, *6*, 19371−19380.
(19) Sihtola, H. Chemical Properties of Modified Celluloses. *Die Makromol. Chemie* **1959**, *35*, 250−265.
(20) Spedding, H. 628. Infrared Spectra of Periodate-Oxidised Cellulose. *J. Chem. Soc.* **1960**, 3147.
(21) Erlandsson, J.; López Durán, V.; Granberg, H.; Sandberg, M.; Larsson, P. A.; Wågberg, L. Macro- and Mesoporous Nanocellulose Beads for Use in Energy Storage Devices. *Appl. Mater. Today* **2016**, *5*, 246−254.
(22) Kim, U.-J.; Wada, M.; Kuga, S. Solubilization of Dialdehyde Cellulose by Hot Water. *Carbohydr. Polym.* **2004**, *56*, 7−10.
(23) Larsson, P. A.; Berglund, L. A.; Wågberg, L. Ductile All-Cellulose Nanocomposite Films Fabricated from Core−Shell Structured Cellulose Nanofibrils. *Biomacromolecules* **2014**, *15*, 2218−2223.
(24) Liimatainen, H.; Visanko, M.; Sirviö, J. A.; Hormi, O. E. O.; Niinimaki, J. Enhancement of the Nanofibrillation of Wood Cellulose through Sequential Periodate−Chlorite Oxidation. *Biomacromolecules* **2012**, *13*, 1592−1597.
(25) Sirvio, J.; Hyvakko, U.; Liimatainen, H.; Niinimaki, J.; Hormi, O. Periodate Oxidation of Cellulose at Elevated Temperatures Using Metal Salts as Cellulose Activators. *Carbohydr. Polym.* **2011**, *83*, 1293−1297.
(26) Yang, X.; Cranston, E. D. Chemically Cross-Linked Cellulose Nanocrystal Aerogels with Shape Recovery and Superabsorbent Properties. *Chem. Mater.* **2014**, *26*, 6016−6025.
(27) Larsson, P. A.; Wågberg, L. Towards Natural-Fibre-Based Thermoplastic Films Produced by Conventional Papermaking. *Green Chem.* **2016**, *18*, 3324−3333.
(28) Matsumura, H.; Sugiyama, J.; Glasser, W. G. Cellulosic Nanocomposites. I. Thermally Deformable Cellulose Hexanoates from Heterogeneous Reaction. *J. Appl. Polym. Sci.* **2000**, *78*, 2242−2253.
(29) Kim, U.-J.; Kuga, S.; Wada, M.; Okano, T.; Kondo, T. Periodate Oxidation of Crystalline Cellulose. *Biomacromolecules* **2000**, *1*, 488−492.
(30) Kristiansen, K. A.; Potthast, A.; Christensen, B. E. Periodate Oxidation of Polysaccharides for Modification of Chemical and Physical Properties. *Carbohydr. Res.* **2010**, *345*, 1264−1271.
(31) Karlsson, R.-M. P.; Larsson, P. T.; Yu, S.; Pendergraph, S. A.; Pettersson, T.; Hellwig, J.; Wågberg, L. Carbohydrate Gel Beads as Model Probes for Quantifying Non-Ionic and Ionic Contributions behind the Swelling of Delignified Plant Fibers. *J. Colloid Interface Sci.* **2018**, *519*, 119−129.
(32) Grignon, J.; Scallan, A. M. Effect of PH and Neutral Salts upon the Swelling of Cellulose Gels. *J. Appl. Polym. Sci.* **1980**, *25*, 2829−2843.
(33) Fukuzumi, H.; Saito, T.; Isogai, A. Influence of TEMPO-Oxidized Cellulose Nanofibril Length on Film Properties. *Carbohydr. Polym.* **2013**, *93*, 172−177.
(34) Puangsin, B.; Yang, Q.; Saito, T.; Isogai, A. Comparative Characterization of TEMPO-Oxidized Cellulose Nanofibril Films Prepared from Non-Wood Resources. *Int. J. Biol. Macromol.* **2013**, *59*, 208−213.
(35) Plappert, S. F.; Nedelec, J.-M.; Rennhofer, H.; Lichtenegger, H. C.; Liebner, F. W. Strain Hardening and Pore Size Harmonization by Uniaxial Densification: A Facile Approach toward Superinsulating Aerogels from Nematic Nanofibrillated 2,3-Dicarboxyl Cellulose. *Chem. Mater.* **2017**, *29*, 6630−6641.
(36) O'Meara, D.; Richards, G. N. 909. Alkaline Degradation of Polysaccharides. Part V. Periodate Oxycellulose. *J. Chem. Soc.* **1958**, 4504.
(37) Fält, S.; Wågberg, L.; Vesterlind, E.-L. Swelling of Model Films of Cellulose Having Different Charge Densities and Comparison to the Swelling Behavior of Corresponding Fibers. *Langmuir* **2003**, *19*, 7895−7903.
(38) Gellerstedt, F.; Wågberg, L.; Gatenholm, P. Swelling Behaviour of Succinylated Fibers. *Cellulose* **2000**, *7*, 67−86.
(39) Guthrie, R. D. The "Dialdehydes" from the Periodate Oxidation of Carbohydrates. *Adv. Carbohydr. Chem.* **1962**, *16*, 105−158.

https://dx.doi.org/10.1021/acs.biomac.0c00040
Biomacromolecules 2020, 21, 1480−1488

(40) Codou, A.; Guigo, N.; Heux, L.; Sbirrazzuoli, N. Partial Periodate Oxidation and Thermal Cross-Linking for the Processing Ofthermosetall-Cellulose Composites. *Compos. Sci. Technol.* **2015**, *117*, 54−61.
(41) Potthast, A.; Schiehser, S.; Rosenau, T.; Kostic, M. Oxidative Modifications of Cellulose in the Periodate System − Reduction and Beta-Elimination Reactions 2nd ICC 2007, Tokyo, Japan, October 25−29, 2007. *Holzforschung* **2009**, *63*, 12−17.
(42) Morooka, T.; Norimoto, M.; Yamada, T. Periodate Oxidation of Cellulose by Homogeneous Reaction. *J. Appl. Polym. Sci.* **1989**, *38*, 849−858.
(43) Fujisawa, S.; Okita, Y.; Fukuzumi, H.; Saito, T.; Isogai, A. Preparation and Characterization of TEMPO-Oxidized Cellulose Nanofibril Films with Free Carboxyl Groups. *Carbohydr. Polym.* **2011**, *84*, 579−583.
(44) Syverud, K.; Stenius, P. Strength and Barrier Properties of MFC Films. *Cellulose* **2009**, *16*, 75−85.
(45) Aulin, C.; Gällstedt, M.; Lindström, T. Oxygen and Oil Barrier Properties of Microfibrillated Cellulose Films and Coatings. *Cellulose* **2010**, *17*, 559−574.
(46) Fukuzumi, H.; Saito, T.; Iwata, T.; Kumamoto, Y.; Isogai, A. Transparent and High Gas Barrier Films of Cellulose Nanofibers Prepared by TEMPO-Mediated Oxidation. *Biomacromolecules* **2009**, *10*, 162−165.
(47) Wang, H.; Li, D.; Zhang, R. Preparation of Ultralong Cellulose Nanofibers and Optically Transparent Nanopapers Derived from Waste Corrugated Paper Pulp. *BioResources* **2013**, *8*, 1374−1384.
(48) Sehaqui, H.; Liu, A.; Zhou, Q.; Berglund, L. A. Fast Preparation Procedure for Large, Flat Cellulose and Cellulose/Inorganic Nanopaper Structures. *Biomacromolecules* **2010**, *11*, 2195−2198.
(49) Larsson, P. A.; Kochumalayil, J. J.; Wågberg, L. Oxygen and Water Vapour Barrier Films with Low Moisture Sensitivity Fabricated from Self-Crosslinking Fibrillated Cellulose. *15th Fundamental Research Symposium: Advanced in Pulp and Paper Research*, 2013; Vol. *134* (16), pp 851−866.
(50) Larsson, P. A.; Pettersson, T.; Wågberg, L. Improved Barrier Films of Cross-Linked Cellulose Nanofibrils: A Microscopy Study. *Green Mater.* **2014**, *2*, 163.
(51) Li, Z.; Liu, W.; Guan, F.; Li, G.; Song, Z.; Yu, D.; Wang, H.; Liu, H. Using Cellulose Fibers to Fabricate Transparent Paper by Microfibrillation. *Carbohydr. Polym.* **2019**, *214*, 26−33.
(52) Liimatainen, H.; Visanko, M.; Sirviö, J.; Hormi, O.; Niinimäki, J. Sulfonated Cellulose Nanofibrils Obtained from Wood Pulp through Regioselective Oxidative Bisulfite Pre-Treatment. *Cellulose* **2013**, *20*, 741−749.

https://dx.doi.org/10.1021/acs.biomac.0c00040
Biomacromolecules 2020, 21, 1480−1488